This article has been accepted for inclusion in a future issue of this journal. Content is final as presented, with the exception of pagination.

Performance Analysis of Models for Calculating the Maximum Power of High Concentrator Photovoltaic Modules

Alberto Soria-Moya, Florencia Almonacid Cruz, Eduardo F. Fernández, Pedro Rodrigo, Tapas K. Mallick, *Member, IEEE*, and Pedro Pérez-Higueras

***Abstract*—Due to its special features, one of the problems of high concentrator photovoltaic (HCPV) technology is the estimation of the electrical output of an HCPV module. Although there are several methods for doing this, only some of them can be applied using easily obtainable atmospheric parameters. In this paper, four models to estimate the maximum power of an HCPV module are studied and compared. The models that have been taken into account are the standard ASTM E2527, the linear coefficient model, the Sandia National Laboratories model, and an artificial neural network-based model. Results demonstrate that the four methods show adequate behavior in the estimation of the maximum power of several HCPV modules from different manufacturers.**

***Index Terms*—High concentrator photovoltaic (HCPV), mathematical methods, maximum power, outdoor measurements.**

I. Introduction

AFTER more than 30 years of research into high concentrator photovoltaics (HCPV), this technology is finally entering the market [1], [2]. Although this technology has not achieved yet the needed momentum, HCPV could be in the power generation market soon because of the high efficiencies already reached and expected for this technology [3]–[8].

HCPV cells and modules operate under concentrations between 300 and 2000 suns. This technology is based on optical devices that focus the light received from the sun on the solar cell surface. A typical HCPV module is composed of multijunction (MJ) solar cells, usually monolithic lattice-matched GaInP/GaInAs/Ge III–V triple-junction solar cells, interconnected in series with one optical device per cell, as well as a Fresnel lens and a secondary optical element that concentrates the light with a ratio of around 500–1000 suns [9]. MJ concentrator solar cells are influenced by changes in irradiance, spectrum, and temperature [10]–[12]. Due to the use of these kinds of cells and optical elements, the performance of HCPV modules are also going to be mainly affected by these parameters [13]–[16].

While there is much experience in the modeling of conventional photovoltaic modules with comparisons among different models having been done, there is a little experience in these kinds of studies in HCPV. Therefore, these kinds of studies present great interest and novelty for HCPV technology. Because of these special features, one of the problems of HCPV technology is the difficulty of finding simple and accurate methods that allow prediction of the output of an HCPV module under real conditions. There are several methods for the estimation of the maximum power of an HCPV module. These models present different levels of complexity and accuracy and require different equipment to be applied [17]. The aim of this paper is to study and compare some of these models. In particular, the models used will be those that estimate the maximum power of an HCPV module from outdoor measurements easy to get or estimate from atmospheric databases in order to facilitate their application. Taking this into account, the only models consider have been the standard ASTM E2527 model [18], the linear coefficient model [19], the Sandia National Laboratories model [20], and an artificial neural network (ANN)-based model [21]. The most of the other methods usually need measurements of specific instruments, detailed information of the materials of the modules which is not always available, and advanced knowledge of semiconductor physics, optics, or different specific software. The analysis and comparison of these models for the prediction of the maximum power of HCPV modules in outdoor conditions is useful to promote this technology. Furthermore, the coefficients of all the studied models for several modules are given in order to have a reference of these values of current HCPV modules. This also allows the application of each model for the modules under study.

This paper is organized as follows. Section II describes the experimental setup used to measure and study the HCPV module. In Section III, the descriptions of the models and results obtained in the estimation of maximum power of HCPV modules under study are presented and commented on. In Section IV,

Manuscript received October 3, 2014; accepted January 25, 2015. This work was supported by the Engineering and Physical Sciences Research Council through the BioCPV (EP/J000345/1) project. This work is part of the project "Desenvolvemento de novos conceptos baseados en tecnoloxía de concentración fotovoltaica para a produción de enerxía eléctrica adaptados a distintas zonas climáticas," through the program "formación posdoutoral do Plan galego de investigación, innovación e crecemento 2011–2015 (Plan I2C)" funded by the Xunta de Galicia and by the European Social Fund.

A. Soria-Moya, F. Almonacid Cruz, and P. Pérez-Higueras are with the Centre of Advanced Studies in Energy and Environment, University of Jaén, Jaén 23071, Spain (e-mail: tecnico@censolar.org; facruz@ujaen.es; pjperez@ujaen.es).

E. F. Fernández is with the Centre of Advanced Studies in Energy and Environment, University of Jaén, Jaén 23071, Spain, and also with the Environment and Sustainability Institute, University of Exeter, Penryn TR10 9FE, U.K. (e-mail: fenandez@ujaen.es).

P. Rodrigo is with Panamericana University, Aguascalientes 20290, Mexico (e-mail: prodrigo@up.edu.mx).

T. K. Mallick is with the Environment and Sustainability Institute, University of Exeter, Penryn TR10 9FE, U.K. (e-mail: T.K.Mallick@exeter.ac.uk).

Color versions of one or more of the figures in this paper are available online at http://ieeexplore.ieee.org.

Digital Object Identifier 10.1109/JPHOTOV.2015.2397605

TABLE I
MAXIMUM POWER OF THE MODULES UNDER STUDY MEASURED AT THE SAME OUTDOOR REFERENCE CONDITIONS FOR WIND SPEED LOWER THAN 1 M/S

Manufacturer	P (W)	DNI (W/m^2)	$T_{\rm air}$ (°C)	AM
A	57.2	900	20	1.5
B	116.9	900	20	1.5
C	45.7	900	20	1.5

P: Maximum power. DNI: Direct normal irradiance. $T_{\rm air}$: Air temperature. AM: Air mass.

a comparative study among the models used is presented. The main conclusions of the work are presented in Section V.

II. EXPERIMENTAL SETUP

To conduct this study, three HCPV modules from different manufacturers have been selected. These modules are representative of the current industrialized modules, but for confidentiality reasons, they are named as module A, module B, and module C, respectively. The three modules are made of lattice-matched GaInP/GaInAs/Ge MJ solar cell, a PMMA Fresnel lens as primary optic, and a refractive truncated pyramid as secondary optic. Module A has a geometric concentration of 500 and six cells connected in series. Module B has a geometric concentration of 550 and 25 cells connected in series. Module C has a geometric concentration of 625 and five cells connected in series. All of them have a passive cooling. Table I shows the maximum power of the modules under study, measured at the same outdoor reference conditions, obtained following the procedure described in [13].

HCPV modules were measured at the Centre of Advanced Studies in Energy and Environment (CEAEMA), University of Jaén. The center is located at the south of Spain, Jaén, which has a high direct annual irradiation level [22] and air temperatures that can easily reach 40 °C in summer and 5 °C in winter. Because of this, the solar research center is located in an adequate place for HCPV outdoor evaluation.

To carry out this study, the modules were mounted on a high-accuracy two-axis solar tracker. The *I–V* characteristics of the modules were measured with a four-wire electronic load. In addition, a four-wire PT100 placed in contact with the solar cell on the concentrator receiver for each module to measure the cell temperature was installed. It is important to note that each temperature sensor was located in a receiver between the center and the border of the modules so that the measured temperatures should be considered as the average temperature of a receiver due to the temperature distribution of HCPV modules. This approach has been previously used and has been considered as a useful tool for the estimation of the cell temperature of an HCPV module and for its electrical characterization [23]–[25]. An atmospheric station recorded other outdoor parameters such as global irradiance (G), direct normal irradiance (DNI), wind speed ($W_{\rm s}$), air temperature ($T_{\rm air}$), relative humidity ($H_{\rm r}$), or sun elevation ($\gamma_{\rm s}$), among others.

Fig. 1 shows the experimental setup to study the behavior of the HCPV modules described above. All the parameters were recorded every 5 min from January 2011 to December 2012. It is also important to note that the modules were cleaned once a week and also after rainy days to avoid possible power losses.

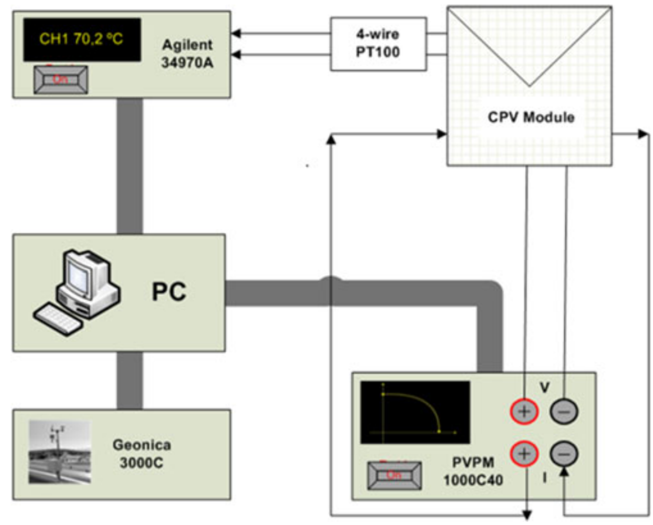

Fig. 1. Scheme of the experimental setup used to study the HCPV modules' behavior at the CEAEMA of the University of Jaén.

Since the MJ solar cells and the HCPV modules are influenced by the incident spectrum, some of the methods that will be studied in next sections use different atmospheric parameters to evaluate its impact. As will be commented, the parameters used are the air mass (AM) and the precipitable water (PW). These parameters are not directly given by the atmospheric station but can be easily calculated. In this case, AM has been determined knowing $\gamma_{\rm s}$ [26] and PW knowing $T_{\rm air}$ and H_r [27], [28].

Fig. 2 shows the distribution of the main annual atmospheric parameters measured during the experiment at Jaén.

III. HIGH CONCENTRATOR PHOTOVOLTAIC MODULE METHODS

In this section, the models that have been considered will be described and studied. Particularly, the considered models are the standard ASTM E2527 model [18], the linear coefficient model [19], the Sandia National Laboratories model [20], and an ANN-based model [21]. The parameters of each model considered have been obtained from outdoor monitorized data and following the procedure described for each author.

A. *Model of the Standard ASTM E2527*

The American standard ASTM E2527 [18] defines a simple procedure to predict the maximum power of an HCPV module. The proposed equation is

$$P_{\rm ASTM} = {\rm DNI} \cdot (A_1 + A_2 \cdot {\rm DNI} + A_3 \cdot T_{\rm air} + A_4 \cdot W_s) \tag{1}$$

where A_1, A_2, A_3, and A_4 coefficients are estimated by means of regression analysis from outdoor monitorized data following the procedure described by the authors. Table II shows the values of the coefficients for each module under study. As can be seen, although the HCPV module is influenced by spectral

This article has been accepted for inclusion in a future issue of this journal. Content is final as presented, with the exception of pagination.

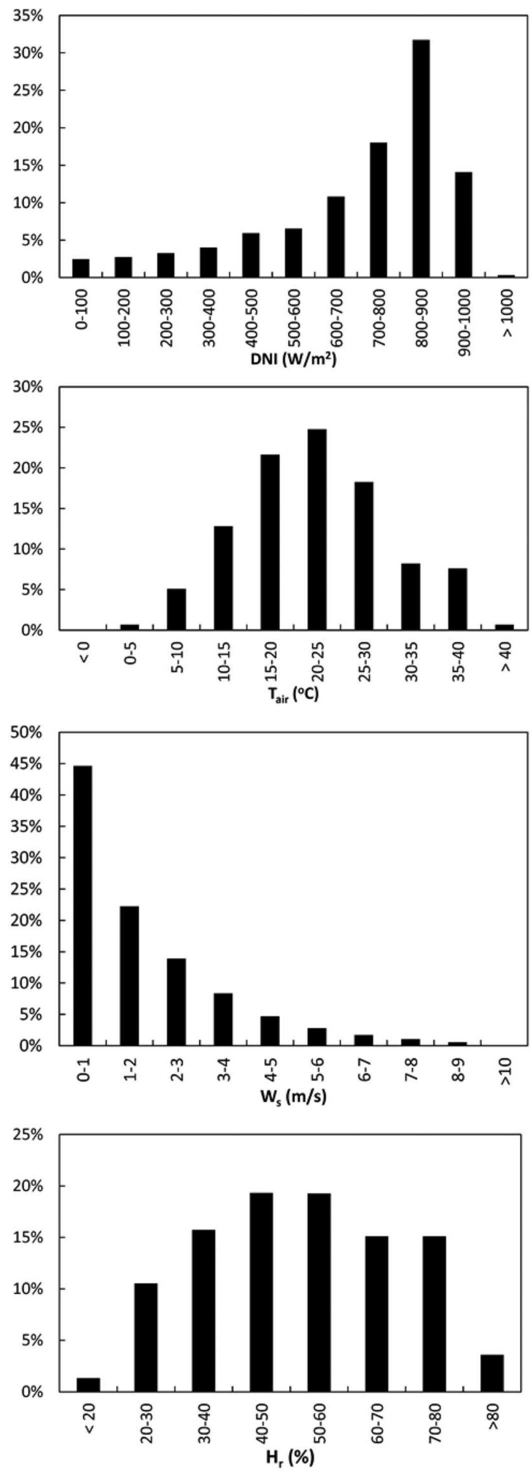

Fig. 2. Distribution of DNI, $T_{\rm air}$, $W_{\rm s}$, and $H_{\rm r}$ values measured during the experiment.

changes, this model does not take into account any spectral correction.

B. Model Based on Linear Coefficients

The linear coefficient model [19], [29] uses input parameters DNI, $T_{\rm air}$, and AM to quantify the spectral influences on the HCPV module. The equation of the model to obtain the maximum power of a HCPV module is

$$P_{\rm Linear} = \frac{P^+}{\mathrm{DNI}^+}\mathrm{DNI}(1-\delta(T_{\rm air}-T^+_{\rm air}))(1-\varepsilon(\mathrm{AM}-\mathrm{AM}_U)) \qquad (2)$$

where P^+, DNI^+, $T_{\rm air}$ are, respectively, the maximum power, direct normal irradiance, and air temperature at reference conditions (see Table I); δ is the air temperature coefficient of maximum power; ε is the AM coefficient of maximum power of an HCPV module (its value being 0 for $\mathrm{AM} \leq \mathrm{AM_U}$ and the value obtained by the regression analysis of outdoor monitored data for $\mathrm{AM} > \mathrm{AM_U}$); and $\mathrm{AM_U}$ is defined as the umbral AM at which the maximum power begins to be influenced, where its value is about 2, as has been found in [16], [19], and [30].

The temperature coefficients of maximum power (δ) and AM coefficients of maximum power (ε) for the HCPV modules under study are obtained from outdoor monitorized data by means of regression analysis following the procedure described by the authors; results are shown in Table III.

TABLE II
COEFFICIENTS OBTAINED FOR THE THREE MODULES UNDER STUDY OF THE ASTM E2527 MODEL

	A_1	A_2	A_3	A_4
A	3.60905E-02	2.76245E-05	1.42270E-04	2.13138E-04
B	9.56743E-02	3.34642E-05	1.11243E-04	8.00692E-04
C	3.24868E-02	1.61190E-05	0.85932E-04	4.85177E-04

TABLE III
TEMPERATURE COEFFICIENTS OF MAXIMUM POWER (δ) AND AM COEFFICIENTS OF MAXIMUM POWER (ε) OBTAINED FOR THE THREE HCPV MODULES UNDER STUDY OF THE LINEAR COEFFICIENT MODEL

Manufacturer	δ (%/°C)	ε (%)	
		$\mathrm{AM} \leq \mathrm{AM_U}$	$\mathrm{AM} > \mathrm{AM_U}$
A	0.14	0	4.74
B	0.12	0	4.11
C	0.17	0	4.80

C. Model of Sandia National Laboratories

The model of Sandia National Laboratories [20] uses the DNI, the AM and the $T_{\rm cell}$ as inputs. The equations that allow calculating the HCPV module maximum power are

$$f_1\,(\mathrm{AM}) = a_0 + a_1\cdot \mathrm{AM} + a_2\cdot \mathrm{AM}^2 + a_3\cdot \mathrm{AM}^3 + a_4\cdot \mathrm{AM}^4 \qquad (3)$$

$$B_{\rm ef}\,(\mathrm{AM}) = (\mathrm{DNI}\cdot f_1\,(\mathrm{AM}))\,\mathrm{DNI}^* \qquad (4)$$

$$\delta = (m\cdot k\cdot (T_{\rm cell}+273.15))/q \qquad (5)$$

$$\beta_{V\,{\rm mpp}} = \beta_{V\,{\rm mpp0}} + m_{V\,{\rm mpp}}\cdot (1-B_{\rm ef}) \qquad (6)$$

$$I_{\rm mpp} = \left(C_0\cdot B_{\rm ef} + C_1\cdot B^2_{\rm ef}\right) \times \left(I^*_{\rm mpp} + \alpha_{\rm Impp}\cdot (T_{\rm cell}-T^*_{\rm cell}\right) \qquad (7)$$

TABLE IV
PARAMETERS OBTAINED FOR THE THREE MODULES UNDER STUDY OF THE MODEL OF SANDIA NATIONAL LABORATORIES

Parameter	A	B	C	Units
α_{Impp}	0.0077	0.0009	0.0083	A/°C
$\beta_{\mathrm{Vmpp}}0$	−0.049	−0.140	−0.029	V/°C
$m_{V\,\mathrm{mpp}}$	−0.002	−0.004	−0.001	V/°C
a_0	1.0185	0.8841	0.8991	–
a_1	0.00198	0.08849	0.09765	–
a_2	−0.0127	−0.0279	−0.0294	–
a_3	0.00102	0.00201	0.00210	–
a_4	−2.367E-5	−4.575E-5	−4.769E-5	–
I^*_{mpp}	4.12	2.37	4.24	A
V^*_{mpp}	15.92	60.91	12.22	V
m	1.14	5.12	5.59	–
C_0	1.018	0.928	0.950	–
C_1	−0.018	0.072	0.050	–
C_2	−4.33	−0.20	−0.15	–
C_3	−48.93	−1.28	−0.98	1/V

$$\begin{aligned} V_{\mathrm{mpp}} = {} & V^*_{\mathrm{mpp}} + C_2 \cdot N_S \cdot \delta \cdot \ln\left(B_{\mathrm{ef}}\right) \\ & + C_3 \cdot N_S \cdot \left(\delta \cdot \ln\left(B_{\mathrm{ef}}\right)\right)^2 \\ & + \beta_{V\,\mathrm{mpp}} \cdot \left(T_{\mathrm{cell}} - T^*_{\mathrm{cell}}\right) \end{aligned} \quad (8)$$

$$P_{\mathrm{Sandia}} = I_{\mathrm{mpp}} \cdot V_{\mathrm{mpp}}. \quad (9)$$

Equation (3) approximates the spectral correction factor $f_1(\mathrm{AM})$, as defined in the standard ASTM E 973 [31], by a fourth-order polynomial. Equation (4) calculates the effective irradiance (B_{ef}), that is, the irradiance at which the cells actually respond. This irradiance is the DNI corrected with the spectral correction factor, $f_1(\mathrm{AM})$, and normalized to the reference irradiance, DNI*. Equation (5) defines the δ parameter, which is the product of the effective ideality factor of the MJ cell (m) and the thermal voltage. The thermal voltage is obtained from the Boltzmann constant (k), the electron charge (q), and the cell temperature. Equation (6) allows the determination of the temperature coefficient $\beta_{V\,\mathrm{mpp}}$. This coefficient is used afterward for quantifying the effect of temperature on the module maximum power point voltage. The coefficient is expressed as a linear function of the effective irradiance, i.e., it is allowed to vary with the concentration ratio. Equations (7) and (8) calculate the module maximum power point current (I_{mpp}) and voltage (V_{mpp}) from their values at reference conditions (I^*_{mpp}, V^*_{mpp}). $\alpha_{I\mathrm{mpp}}$ is the temperature coefficient for I_{mpp}, and N_{S} is the number of cells in series for the module. Finally, (9) obtains the maximum power of the HCPV module. The reference conditions are defined as: DNI* $= 1000$ W/m^2, $T^*_{\mathrm{cell}} = 25$ °C and AM1.5. Every model parameter is obtained from outdoor monitorized data by means of regression analysis, following the procedures described by the authors; results are shown in Table IV.

D. Model Based on Artificial Neural Network

Due to the fact that the relation between atmospheric parameters and module output maximum power is complex, a model that tries to characterize the relation between atmospheric parameters and module output maximum power through ANNs has been proposed in [21]. The model takes into account the spectral influences through easily measurable parameters: the AM and the PW. Inputs of the model are the DNI, the T_{air}, the W_{s}, the AM, and the PW. Therefore, the maximum power is defined by the following function:

$$P_{\mathrm{ANN}} = f\left(\mathrm{DNI}, \mathrm{AM}, \mathrm{PW}, T_{\mathrm{air}}, W_s\right). \quad (10)$$

To estimate this function, a feed-forward neural network trained with the Levenberg–Marquardt (LM) back-propagation algorithm was used. The developed ANN has the structure shown in Fig. 3: five nodes in the input layer (DNI, AM, PW, T_{air}, W_{s}), seven nodes in the hidden layer, and one node in the output layer: the maximum power. The number of hidden layer nodes was determined empirically [32]–[35]. To find the final architecture (weights and bias and the number of nodes in the hidden layer), several ANNs with different structures were trained in order to find the ANN that best fitted the network output to the target. The LM training algorithm was used to adjust the weights and bias such that the neural network produces the required output for the given inputs data [36]–[38]. In order to train, validate, and test the ANN, a set of outdoor measurements were used for a wide range of operating conditions following the procedure described by the authors.

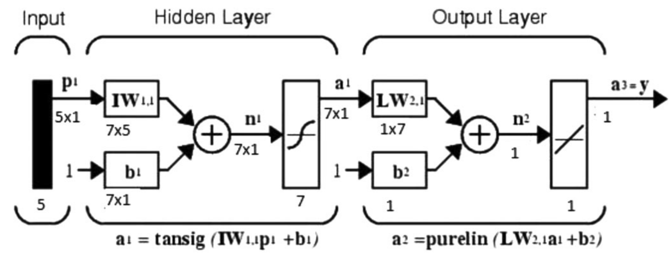

Fig. 3. Structure of the ANN for the prediction of the maximum power of an HCPV module.

TABLE V
CONFIGURATION AND TRAINING PERFORMANCE OF ANN FOR ESTIMATING THE OUTPUT OF THREE MODULES UNDER STUDY

Programing Language	MATLAB 2011b$^{\mathrm{T}}$
Neurons inputs	3
Neurons output layer	1
Neuron hidden layer	5
Maximum iteration limits	500
Training function	Levenberg–Marquardt
Performance function	Mean Square Error
Performance goal	1.00e^{-010}
Minimum gradient	1.00e^{-05}

Table V shows the configuration and main features of the ANN used to estimate the output of the HCPV modules considered. Tables VI and VII show values of weight and bias for the hidden and output layer neurons obtained for the studied modules.

IV. COMPARATIVE STUDY

To study the behavior of the presented models in detail, the root mean square error (RMSE), the mean bias error (MBE),

This article has been accepted for inclusion in a future issue of this journal. Content is final as presented, with the exception of pagination.

TABLE VI
VALUES OF WEIGHTS AND BIAS OBTAINED FOR THE HIDDEN LAYER NEURONS FOR THREE MODULES UNDER STUDY

	Hidden layer					
	Bias	Weights				
A	−1.8429	2.5940	2.2913	2.0389	0.9202	0.2399
	12.7312	−1.1261	−18.5147	−2.7033	0.3902	−0.3920
	−0.7949	0.3861	0.0269	−0.1795	0.0312	0.0682
	2.6424	−2.0327	−1.7782	−1.0675	−0.6628	−0.1742
	−9.2255	−8.7349	13.4286	−5.9909	15.7909	−0.5748
	−1.6165	1.0121	−0.0637	−1.0271	0.1804	0.3708
	1.8776	2.0357	0.5695	1.6886	0.7943	-1.0422
B	−0.0333	−0.8164	−0.0158	0.1841	0.0311	−0.0203
	5.1063	0.8322	−0.3461	5.8053	−1.3989	0.0735
	0.0492	−1.6218	−0.3890	−1.4026	−1.8233	0.7208
	0.8378	−0.2589	−0.4826	0.2493	−0.6977	−2.1617
	0.3880	−1.4806	−0.4486	0.7209	−0.0565	−1.3546
	−2.5878	1.9492	−0.8359	−1.3351	0.1719	1.3480
	1.3662	2.7184	0.9630	−1.3420	−1.1131	1.68329
C	−3.5358	−0.5130	−0.1083	−2.9562	0.6337	−2.4696
	−0.0284	−1.5463	−0.3744	−3.8941	−8.0610	6.2506
	0.8811	−0.7570	−0.0183	−0.0592	0.1353	0.0915
	−1.2296	−1.7805	−0.2535	−2.0785	0.1738	−0.3308
	−0.9498	0.3862	0.0077	−0.2388	−0.0352	−0.0522
	−4.0959	−0.0648	0.4302	−3.0006	0.3828	−0.0756
	4.2547	−0.1722	−2.1945	2.6365	1.1541	0.7253

TABLE VII
VALUES OF WEIGHTS AND BIAS OBTAINED FOR THE OUTPUT LAYER NEURONS FOR THREE MODULES UNDER STUDY

	Output layer							
	Bias	Weights						
A	−2.73	2.73	0.06	4.51	7.67	−0.02	−0.56	0.130
B	−0.14	−1.10	0.14	−0.12	0.07	−0.05	0.113	0.203
C	1.065	−0.08	−0.03	3.42	−0.24	8.02	−2.030	−0.169

TABLE VIII
RMSE, MBE, AND DETERMINATION COEFFICIENT (R^2) OBTAINED FOR THE STUDIED MODELS

	Model	RMSE (%)	MBE (%)	R^2
A	Standard ASTM E2527	4.59	0.00	0.97
	Linear Coefficients	3.22	0.05	0.99
	Sandia National Laboratories	3.35	−0.05	0.99
	Artificial Neural Network	2.11	0.00	0.99
B	Standard ASTM E2527	4.50	0.00	0.97
	Linear Coefficients	3.48	−0.07	0.99
	Sandia National Laboratories	3.60	−0.09	0.99
	Artificial Neural Network	1.96	-0.07	0.99
C	Standard ASTM E2527	5.20	0.00	0.96
	Linear Coefficients	3.55	0.03	0.98
	Sandia National Laboratories	3.60	−0.08	0.98
	Artificial Neural Network	2.56	−0.05	0.98

and the value of determination coefficient (R^2) between predicted and actual data have been calculated (see Table VIII). In addition, as an example, Fig. 4 shows the linear regression analysis between actual data and predicted data for the studied models for module A in order to show their performance

As can be seen, the value of R^2 is close to 1 for the studied models, which indicates a good fit for all of them, as shown in Table VIII. The MBE gives an indication on the average deviation of the predicted values from the corresponding measured data. A positive MBE value indicates the amount of overestimation in the predicted data and *vice versa*. As can be seen in Table VIII, the four studied models have an MBE around 0%, what indicates that all the models are not overestimating or underestimating the maximum power of the HCPV modules under study. The RMSE represents a measure of the variation of predicted values around the measured data. As can be seen in Table VIII, the model with a larger RMSE is the standard ASTM E2527, its value being between 4.50% and 5.20%. This is probably because the model does not introduce any spectral correction. The linear coefficient model and the Sandia National Laboratories model yield similar results, i.e., an RSME around 3.5%. As can also be seen, the model based on ANN has the lowest RMSE, its value being between 1.96 and 2.56%. From this analysis, it can also be concluded that the four models perform effectively in the prediction of the maximum power of HCPV modules: the four models have an R^2 equal to or greater than 0.96, an MBE almost equal to 0%, and a maximum RMSE lower than 5.50% which can be considered as an acceptable margin of error.

In order to study the models in more detail, the RMSE versus the main parameters that affect the performance of an HCPV module is calculated: DNI, cell temperature, and spectrum. It is important to note that the spectral effects on the output of an HCPV module are mainly given by the AM, aerosol optical depth, and PW [15], [39]–[41]. However, the aerosol optical depth values were not available during the measurements. Hence, in order to study the quality of the models versus the spectrum, the only atmospheric parameters taken into account are the AM and PW. Fig. 5 shows an example of the performance of the four models versus these parameters for module A. It is important to note that the behavior found for the other two modules yields to the same conclusions commented below.

Fig. 5(a) shows the RMSE for each DNI level. As can be seen, the ANN model shows the best results with an RMSE almost constant, centered around 2%. The linear and Sandia models show similar results. Both models show the poorest results for low DNI levels with a maximum RMSE around 4% and show a tendency to have a better performance as the DNI increases until an RMSE value around 2%. The ASTM model shows the poorest results with a maximum RMSE around 6% and shows no particular trend.

Fig. 5(b) shows the RMSE for each T_{cell} level. As can be seen, the ANN, the linear, and the Sandia models have a similar behavior with an RMSE almost constant for all T_{cell} values. However, the ANN model shows the best results with an RMSE around 2%, while the linear and Sandia models have an RMSE around 3%. Again, the ASTM model shows the poorest results with an RMSE that shows a clear tendency to increase for high T_{cell} values with a maximum around 6%.

Fig. 5(c) and (d) shows the RMSE for each AM and PW level, respectively. Regarding AM, the ANN shows the best results with an RMSE almost constant, centered around 2%. Again, the linear and the Sandia models have a similar behavior with an RMSE that shows a tendency to increase until AM val-

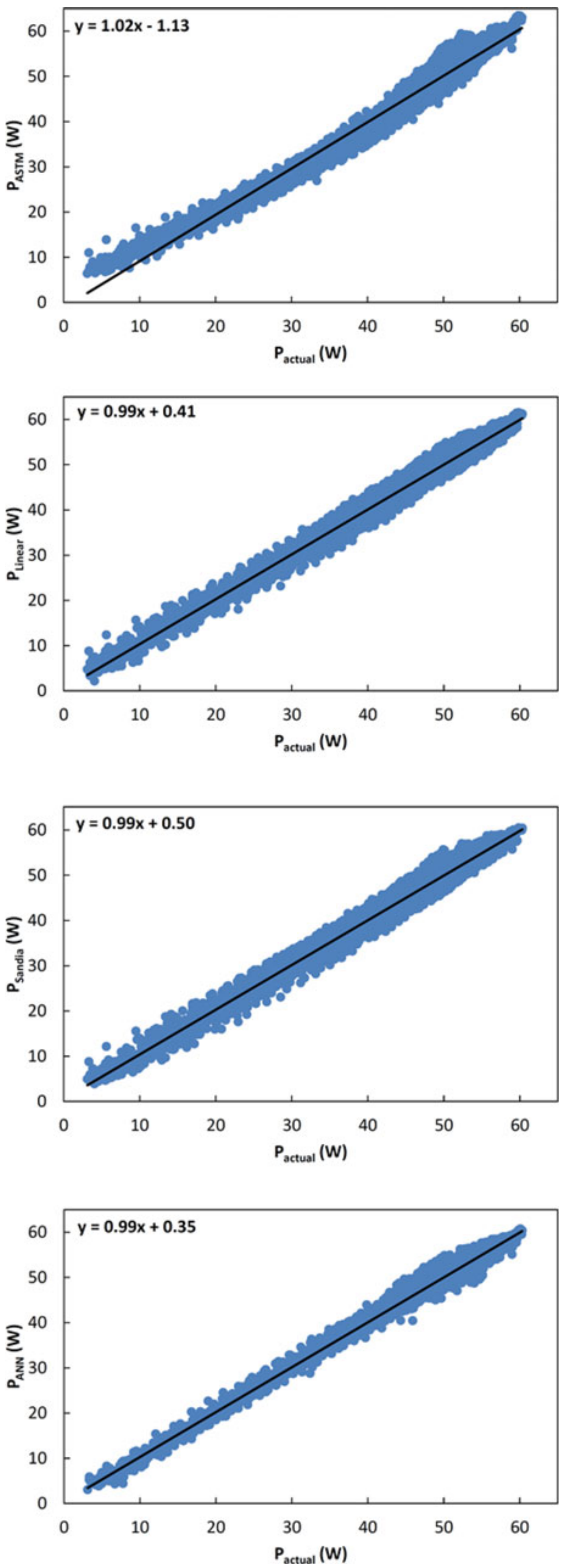

Fig. 4. Linear regression analysis between actual data and predicted data for the studied models for module A.

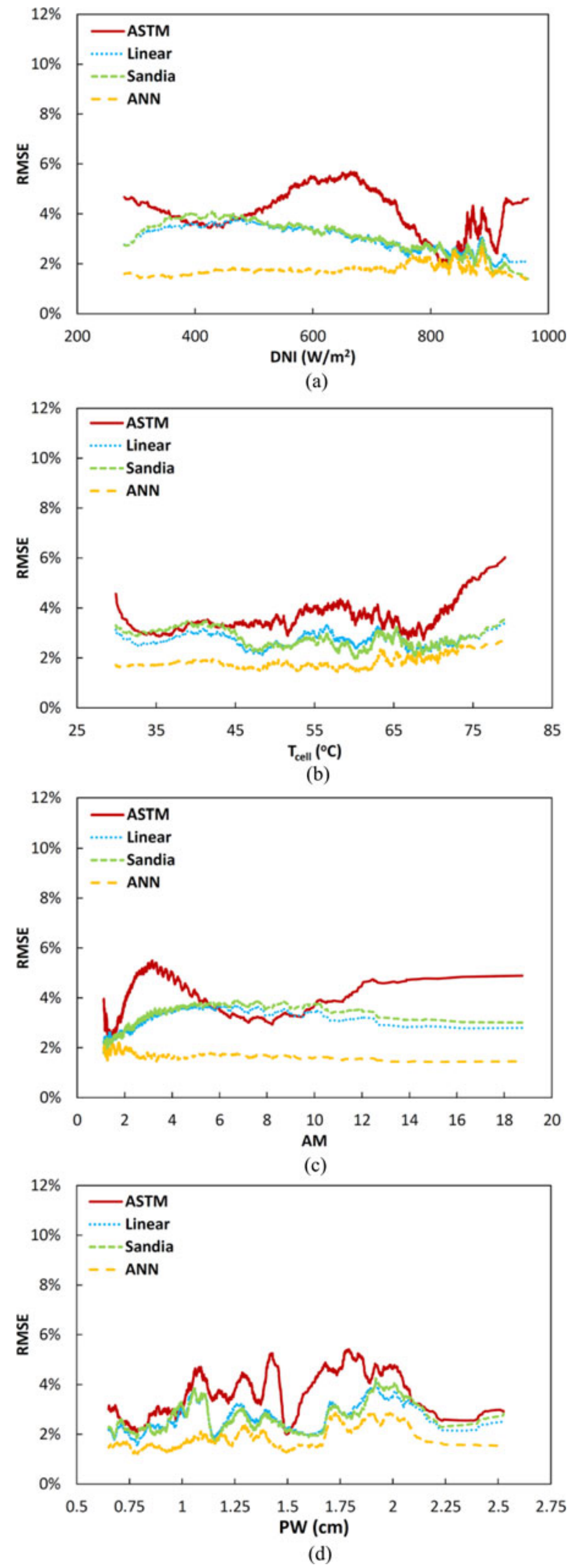

Fig. 5. RMSE for different DNI, T_{cell}, AM, and PW levels for the four studied models for module A.

ues around 5 and keeps almost constant for higher AM values at around 3.5%. The ASTM model shows the poorest results with a maximum RMSE around 5.8% and shows no particular trend. Regarding the PW, all models show the same behavior with a not clear tendency. However, the ANN model provides the best results, while the ASTM model yields the poorest results. The linear and the Sandia models again show similar results.

From the analysis of results, it can be concluded that the model that yields better results is the ANN-based model. This could be explained because the model takes into account a wind speed correction and two spectral corrections (AM and PW) and also to ability of ANN of solving complex problems. However, the model needs advanced knowledge in ANNs. The method based on linear coefficients shows the second best results; furthermore, this model has the advantage that is quite simple to fit and apply. The Sandia National Laboratories model shows a similar behavior to the linear coefficient model. However, this model requires a more complex procedure than other models in order to fit its parameters and needs the cell temperature as input parameter, which is difficult to get, although it is possible to estimate from atmospheric parameters [42]. The ASTM model is also so easy to apply and fit as the linear coefficient model but, because it does not take into account that any spectral correction gives worse results. However, recent works suggest the introduction of spectral correction based on AM and PW in order to improve it [43].

V. Conclusion

A comparative study of four models to estimate the power output of an HCPV module has been undertaken. The studied models estimate the output of HCPV modules from atmospheric parameters that are easy to obtain so that they are useful for a wide variety of HCPV applications. To conduct this study, three HCPV modules from different manufacturers have been selected. These modules are representative of the current industrialized modules; therefore, this study could also allow a further understanding the behavior of this technology in outdoor conditions and promote its application.

From the comparison of the errors of the models, the following conclusions have been found. The ASTM E2527 is the model that gives the poorest results, with an RMSE in the range of 4.50–5.20%. This could be explained because this model does not take into account any spectral correction. The Sandia National Laboratories and the linear coefficient models show similar behavior, with RMSE around 3.5%. The model that shows the best result is the ANN-based model with an RMSE lower than 2.6%. This could be explained because the model includes a wind speed correction and PW as an additional spectral correction. However, results show that the four models can be used to estimate the maximum power of a HCPV module with an RMSE lower than 5%, which can be considered to be an acceptable margin of error. Furthermore, it is important to note that all the models present an MBE around 0%, which means that all of them could be useful to estimate the energy produced by an HCPV module over a year.

In addition, in this paper, all the coefficients obtained for the application of four studied models have been given. This also allows the application of each model for the modules under study. Besides, a significant conclusion could be found from the analysis of coefficients obtained for each model. The coefficients of the ASTM E2527, the Sandia National Laboratories, and the ANNs models have to be considered as fitting parameters without direct physical meaning (with the exception of some coefficients of the Sandia National model). However, the coefficients obtained with the linear model have a physical meaning: relative maximum power losses due to temperature and AM. This means that this model could be used to estimate the maximum power of an HCPV module with similar characteristics to the studied modules, while for the other models, the coefficients need to be adjusted for each different module.

References

[1] M. Robert, “Concentrator photovoltaic technologies: Review and market prospects,” *Refocus*, vol. 6, no. 4, pp. 35–39, 2005.

[2] A. Luque, G. Sala, and I. Luque-Heredia, “Photovoltaic concentration at the onset of its commercial deployment,” *Prog. Photovoltaics, Res. Appl.*, vol. 14, no. 5, pp. 413–428, 2006.

[3] M. Yamaguchi, T. A. K. Takamoto, and N. Ekins-Daukes, “Multi-junction III-V solar cells: Current status and future potential,” *Sol. Energy*, vol. 79, no. 1, pp. 78–85, 2005.

[4] P. Pérez-Higueras, E. Muñoz, G. Almonacid, and P. Vidal, “High concentrator photovoltaics efficiencies: Present status and forecast,” *Renewable Sustainable Energy Rev.*, vol. 15, no. 4, pp. 1810–1815, 2011.

[5] F. Dimroth, M. Grave, P. Beutel, U. Fiedeler, C. Karcher, T. N. D. Tibbits, E. Oliva, G. Siefer, M. Schachtner, A. Wekkeli, A. W. Bett, R. Krause, M. Piccin, N. Blanc, C. Drazek, E. Guiot, B. Ghyselen, T. Salvetat, A. Tauzin, T. Signamarcheix, A. Dobrich, T. Hannappel, and K. Schwarzburg, “Wafer bonded four-junction GaInP/GaAs//GaInAsP/GaInAs concentrator solar cells with 44.7% efficiency,” *Progress Photovoltaics: Res. Appl.*, vol. 22, no. 3, pp. 277–282, 2014.

[6] K. Ghosal, S. Burroughs, K. Heuser, D. Setz, and E. Garralaga-Rojas, “Performance results from micro-cell based high concentration photovoltaic research development and demonstration systems,” *Prog. Photovoltaics, Res. Appl.*, vol. 21, no. 6, pp. 1370–1376, 2013.

[7] K. Ghosal, D. Lilly, J. Gabriel, M. Whitehead, S. Seel, B. Fisher, J. Wilson, and S. Burroughs, “Semprius field results and progress in system development,” *IEEE J. Photovoltaics*, vol. 4, no. 2, pp. 703–708, Mar. 2014.

[8] F. Dimroth, T. Roesener, S. Essig, C. Weuffen, A. Wekkeli, E. Oliva, G. Siefer, K. Volz, T. Hannappel, D. Haussler, W. Jager, and A. Bett, “Comparison of direct growth and wafer bonding for the fabrication of GaInP/GaAs dual-junction solar cells on silicon,” *IEEE J. Photovoltaics*, vol. 4, no. 2, pp. 620–625, Mar. 2014.

[9] A. Luque and V. Andreev, *Concentrator Photovoltaics*. New York, NY, USA: Springer, 2007.

[10] G. Siefer and A. Bett, “Analysis of temperature coefficients for III-V multijunction concentrator cells,” *Prog. Photovoltaics, Res. Appl.*, vol. 22, no. 5, pp. 515–524, 2014.

[11] E. Fernández, G. Siefer, F. Almonacid, A. Loureiro, and P. Pérez-Higueras, “A two subcell equivalent solar cell model for III-V triple junction solar cells under spectrum and temperature variations,” *Sol. Energy*, vol. 92, pp. 221–229, 2013.

[12] E. Fernández, G. Siefer, M. Schachtner, A. García Loureiro, and P. Pérez-Higueras, “Temperature coefficients of monolithic III-V triple-junction solar cells under different spectra and irradiance levels,” in *Proc. AIP Conf.*, 2012, vol. 1477, pp. 189–193.

[13] E. Fernández, P. Pérez-Higueras, A. Garcia Loureiro, and P. Vidal, “Outdoor evaluation of concentrator photovoltaic systems modules from different manufacturers: First results and steps,” *Prog. Photovoltaics, Res. Appl.*, vol. 21, no. 4, pp. 693–701, 2013.

[14] G. Peharz, J. Ferrer Rodríguez, G. Siefer, and A. Bett, “Investigations on the temperature dependence of CPV modules equipped with triple-junction solar cells,” *Prog. Photovoltaics, Res. Appl.*, vol. 19, no. 1, pp. 54–60, 2011.

[15] E. Fernández, F. Almonacid, J. Ruiz-Arias, and A. Soria-Moya, "Analysis of the spectral variations on the performance of high concentrator photovoltaic modules operating under different real climate conditions," *Sol. Energy Mater. Sol. Cells*, vol. 127, pp. 179–187, 2014.
[16] E. Fernández, P. Rodrigo, J. Fernández, F. Almonacid, P. Pérez-Higueras, A. García-Loureiro, and G. Almonacid, "Analysis of high concentrator photovoltaic modules in outdoor conditions: Influence of direct normal irradiance, air temperature, and air mass," *J. Renew. Sustainable Energy*, vol. 6, no. 1, art. no. 013102, 2014.
[17] P. Rodrigo, E. Fernández, F. Almonacid, and P. Pérez-Higueras, "Models for the electrical characterization of high concentration photovoltaic cells and modules: A review," *Renew. Sustainable Energy Rev.*, vol. 26, pp. 752–760, 2013.
[18] *Standard Test Method for Electrical Performance of Concentrator*, ASTM E 2527, 2009.
[19] E. Fernández, F. Almonacid, P. Rodrigo, and P. Pérez-Higueras, "Model for the prediction of the maximum power of a high concentrator photovoltaic module," *Sol. Energy*, vol. 97, pp. 12–18, 2013.
[20] D. L. King, W. E. Boyson, and J. A. Kratochvil, *Photovoltaic Array Performance Model SAND2004–3535*, Sandia Nat. Lab., Albuquerque, NM, USA, 2004.
[21] F. Almonacid, E. F. Fernández, P. Rodrigo, P. Pérez-Higueras, and C. Rus-Casas, "Estimating the maximum power of a high concentrator photovoltaic (HCPV) module using an artificial neural network," *Energy*, vol. 53, pp. 165–172, 2013.
[22] P. Pérez-Higueras, P. Rodrigo, E. Fernández, F. Almonacid, and L. Hontoria, "A simplified method for estimating direct normal solar irradiation from global horizontal irradiation useful for CPV applications," *Renew. Sustainable Energy Rev.*, vol. 16, no. 8, pp. 5529–5534, 2012.
[23] E. Fernández, P. Rodrigo, F. Almonacid, and P. Pérez-Higueras, "A method for estimating cell temperature at the maximum power point of a HCPV module under actual operating conditions," *Sol. Energy Mater. Sol. Cells*, vol. 124, pp. 159–165, 2014.
[24] E. Fernández, F. Almonacid, P. Rodrigo, and P. Pérez-Higueras, "Calculation of the cell temperature of a high concentrator photovoltaic (HCPV) module: A study and comparison of different methods," *Sol. Energy Mater. Sol. Cells*, vol. 121, pp. 144–151, 2014.
[25] P. Rodrigo, E. Fernández, F. Almonacid, and P. Pérez-Higueras, "Review of methods for the calculation of cell temperature in high concentration photovoltaic modules for electrical characterization," *Renew. Sustainable Energy Rev.*, vol. 38, pp. 478–488, 2014.
[26] F. Kasten and A. T. Young, "Revised optical air mass tables and approximation formula," *Appl. Opt.*, vol. 28, no. 22, pp. 4735–4738, 1989.
[27] C. Gueymard, "Assessment of the accuracy and computing speed of simplified saturation vapour equations using a new reference dataset," *J. Appl. Meteorol.*, vol. 32, no. 7, pp. 1294–1300, 1993.
[28] C. Gueymard, "Analysis of monthly average atmospheric precipitable water and turbidity in Canada and northern united states," *Sol. Energy*, vol. 53, no. 1, pp. 57–71, 1994.
[29] E. F. Fernández, F. Almonacid, N. Sarmah, T. Mallick, I. Sanchez, J. M. Cuadra, A. Soria-Moya, and P. Pérez-Higueras, "Performance analysis of the lineal model for estimating the maximum power of a HCPV module in different climate conditions," in *Proc. AIP Conf.*, 2014, vol. 1616, pp. 187–190.
[30] E. Fernández, P. Pérez-Higueras, F. Almonacid, A. García Loureiro, J. Fernández, P. Rodrigo, P. Vidal, and G. Airnonacid, "Quantifying the effect of air temperature in CPV modules under outdoor conditions," in *Proc. AIP*, 2012, vol. 1477, pp. 194–197.
[31] *Determination of the Spectral Mismatch Parameter Between a Photovoltaic Device and a Photovoltaic Reference Cell*, ASTM E 973, 2010.
[32] R. Reed, "Pruning algorithms—A survey," *IEEE Trans. Neural Netw.*, vol. 4, no. 5, pp. 740–747, Sep. 1993.
[33] A. Ghosh and D. Lubkeman, "The classification of power system disturbance waveforms using a neural network approach," *IEEE Trans. Power Del.*, vol. 10, no. 1, pp. 109–115, Jan. 1995.
[34] J. Zurada, *Introduction to Artificial Neural Systems*. Eagan, MN, USA: West, 1992.
[35] B. Curry and P. Morgan, "Model selection in neural networks: Some difficulties," *Eur. J. Oper. Res.*, vol. 170, pp. 567–577, 2004.
[36] K. Levenberg, "A method for the solution of certain problems in least squares," *Quart. Appl. Math.*, vol. 2, pp. 164–168, 1944.
[37] D. Marquardt, "An algorithm for least-squares estimation of nonlinear parameters," *SIAM J. Appl. Math.*, vol. 11, pp. 431–441, 1963.
[38] K. Funahashi, "On the approximate realisation of continuous mappings by neural networks," *Neural Netw.*, vol. 2, pp. 183–192, 1989.
[39] E. F. Fernandez and F. Almonacid, "Spectrally corrected direct normal irradiance based on artificial neural networks for high concentrator photovoltaic applications," *Energy*, vol. 74, pp. 941–949, 2014.
[40] N. Chan, T. B. Young, H. E. Brindley, N. Ekins-Daukes, K. Araki, and Y. Y. Kemmoku, "Validation of energy prediction method for a concentrator photovoltaic module in Toyohashi Japan," *Prog. Photovoltaics, Res. Appl.*, vol. 21, pp. 1598–1610, 2012.
[41] N. Chan, H. Brindley, and N. Ekins-Daukes, "Impact of individual atmospheric parameters on CPV system power, energy yield and cost of energy," *Prog. Photovoltaics, Res. Appl.*, vol. 22, pp. 1080–1095, 2013.
[42] F. Almonacid, P. Pérez-Higueras, E. Fernández, and P. Rodrigo, "Relation between the cell temperature of a HCPV module and atmospheric parameters," *Sol. Energy Mater. Sol. Cells*, vol. 105, pp. 322–327, 2012.
[43] M. Muller, B. Marion, and J. K. S. Rodriguez, "Minimizing variation in outdoor CPV power ratings," in *Proc. AIP Conf.*, 2011, vol. 1407, pp. 336–340

Alberto Soria-Moya received the M.S. degree in physics from University of Seville, Seville, Spain, in 2010. He has been working toward the Ph.D. degree with the University of Jaén, Jaén, Spain, since 2013.

He has been a Researcher with Censolar (Solar Energy Training Centre), Spain, since 2010. From 2008 to 2009, he was a Research Assistant with the Fraunhofer Institute for Solar Energy Systems ISE. His research interests include solar energy, photovoltaics, electrical modeling, and spectral characterization.

Florencia Almonacid Cruz received the M.S. degree in electronic engineering from the University of Granada, Granada, Spain, in 2002 and the Ph.D. degree in electronic engineering from the University of Jaén, Jaén, Spain, in 2009.

She is currently an Associate Professor with the Department of Electronic and Automatic Engineering, University of Jaén. Her research interests include the application of the artificial neural networks in the field of the photovoltaic technology, as well as the characterization and modeling of conventional and concentrator photovoltaic devices and systems.

Eduardo F. Fernández received the B.S. degree in physics from the University of Oviedo, Oviedo, Spain, in 2004 and the M.S. degree in physics, the M.S. degree in renewables energies, and the Ph.D. degree in the area of solar energy from the University of Santiago de Compostela, Santiago de Compostela, Spain, in 2006, 2008, and 2012, respectively.

He is currently a Research Associate with the Environment and Sustainability Institute, University of Exeter, Penryn, U.K., where he is conducting a project funded by the Spanish/Galician government and European Union in the field of concentrator photovoltaics. His research interests include the development, characterization, and modeling of concentrator photovoltaic devices and systems.

Pedro Rodrigo received the M.S. degree in industrial engineering from Navarra University, Pamplona, Spain, in 1998 and the Ph.D. degree in electronic engineering from Jaén University, Jaén, Spain, in 2013.

From 2009 to 2014, he was a Research Assistant with the Center of Advanced Studies in Energy and Environment and with the Solar Energy and Automation Research and Development Group (IDEA), University of Jaén. Since 2014, he has been a Researcher with the Engineering Faculty, Panamericana University, Aguascalientes, México. His research interests include the characterization of concentrator photovoltaic modules and systems.

Tapas K. Mallick (M'14) received the Ph.D. degree from the University of Ulster, Coleraine, U.K., in 2003.

From 2007 to 2012, he was a Lecturer with Heriot-Watt University, Currie, U.K. He is currently a Professor with the Renewable Energy and Chair in Clean Technologies with the Environment and Sustainability Institute, University of Exeter, Penryn, U.K. His research interests include renewable energies, concentrating photovoltaics, building integrated photovoltaics, integration of renewables, heat transfer, optics, and electrical modeling.

Pedro Pérez-Higueras received the Ph.D. degree in industrial engineering from the University of Jaén, Jaén, Spain, in 2003.

He is currently a Professor with the Department of Electronic and Automatic Engineering, University of Jaén. He has collaborated on more than 30 R&D projects with different companies and institutions, and he has published more than 100 papers in the most prestigious peer-reviewed journals and congresses related to solar energy. His research interests include the development, characterization, and modeling of concentrator photovoltaic devices and the optimal design of power plants.